Detailed Description of the Solution

Introduction

In this submission, we describe a phosphorescent panel prototype with honeycomb structure that is embedded with doped strontium aluminate sand. The innovation of our panel design lies in the combination of its unique honeycomb structure and the properties of the phosphorescent material used. This configuration maximizes the surface area available for incorporation of high-performance phosphorescence material compared to traditional flat panels, increases durability, reduces weight, and lowers the cost. Our design is simple: it is a panel with extruded hexagonal (honeycomb) structure with a solid backing on one side. The hexagon walls and the solid backing have a uniform and optimized thickness. The panel shape allows efficient sunlight charging and night emission, and the dimensions allow practical illumination and installation. The housing allows charging during daytime and illuminating the latrines at nighttime, with adjustable light intensity, and illumination area—either inside the latrine or in front of the latrine. The design is effective and meets the solution requirements.

The designed panel can be produced in mass quantities with the low cost and commonly used method of thermoforming—similar to making buckets or car panels. The panels can also be injection molded with plastics of choice, using standard or powder mixing methods and doped strontium aluminate sand. We describe the specific design of the panel and provide results for the prototypes, including the honeycomb design of a 36 cm x 36 cm x 1.4 cm model. We tested our panel with high quality phosphorescent sand with large particle size (500µm). The uniform size and luminosity of the sand allowed us to develop iterations of the prototype with multiple panel dimensions and sand concentrations to optimize the final design solution.

The innovation of our panel design lies in the combination of its unique honeycomb tiles and the properties of the phosphorescent material used. This configuration maximizes the surface area available for incorporation of high-performance phosphorescence material compared to traditional flat panels, increases durability, reduces weight, and lowers the cost. The prototype design is simple and can be injection molded into parts with plastics of choice, using standard or powder mixing methods doped strontium aluminate sand. The phosphorescent sand used in our prototype is chosen for its strong and prolonged luminescence capabilities and heat resistance for injection molding.

The panels can be installed or retrofitted onto latrines. The panel is portable and mountable, optimized to fit and illuminate the latrines, and can be readily deployed as a long-term cost-effective, durable solution for lighting in low-resource settings such as refugee camps. The panels are lightweight and weatherproof. Designed to be easily sanitized, resistant to outdoor elements and deformation and bending after repeated sun exposure and thermal cycling. The housing mechanism is comprised of common construction materials, can be configured to a variety of latrine types and mounting locations, and secured using tamperproof fasteners. The size and dimension of panel is scalable from a pocket or handheld size to larger panels that can be installed into latrines. Multiple panels can also be connected to form multi-directional lanterns.

Our solution integrates the panel embedded with phosphorescent material, its properties, structural housing and other details that meets the solution requirements. We provide a comprehensive design, including structure/housing, rationale/logic, and use case for the phosphorescent panel. This is supported by a detailed study of the properties of the phosphorescent material used, the composition of the panel, and the development and testing of a phosphorescent panel prototype, including iterations of the prototype and other details. Additionally, we describe 3D models of the latrine and prototypes, methods for testing the prototype, lux and light intensity measurements, and the test results. Our submission is a thorough summary of the design, study, and review of the problem, along with proposed solutions based on our phosphorescent panel design and the prototype.

Design Overview

Detailed and Specific Design

We have developed an innovative lighting panel made of plastic embedded with doped strontium aluminate. The panel has a rectangular geometry, measuring 36 cm x 36 cm x 1.4 cm (L x W x H), and consists of a solid, flat backing that is 4 mm high. On top of this backing is a 10 mm high extruded honeycomb pattern. The honeycomb structure has 4 mm thick walls and open hexagonal cells that measure 8 mm across at all parallel faces. The prototype material is clear epoxy resin mixed with phosphorescent sand (500µm particle size doped strontium aluminate) at a 30% concentration. The prototype panel we submitted weighs 1.825 kg. The prototype panel is suitably sized to provide illumination for a latrine throughout the night and to deter theft.

The panel's honeycomb pattern allows it to be easily scaled up or down, and expanded in length, width, or height (Fig. 1A, B). **The housing mechanism for the panel consists of slotted metal framing struts attached to the primary latrine structure (Fig. 1E).** This mechanism secures the phosphorescent panel in the latrine, ensuring theft resistance, easy access for recharging, and versatility in selecting the illumination area. Two variations for securing the panel to the latrine are suggested, both utilizing the same Unistrut metal framing system commonly used for supporting and securing solar panels in place. The suggested framing configuration extends beyond the footprint of the latrine with the panel securely housed in the metal framing slot allowing the panel to be slid outside of the latrine for charging and inside for illumination (Fig. 1C-E). This framing system can also accommodate other illumination sources, including solar or LED lighting. **Figure 2 shows the schematics of the panel and its dimensions and schematics in detail.**

We designed our phosphorescent panel with a hexagonal honeycomb structure and a wall thickness of 4mm to optimize both material usage and performance. The honeycomb design offers several key advantages. First, it provides structural integrity, making the panel more durable and able to withstand environmental conditions. Second, the hexagonal tiling allows for a higher concentration of phosphorescent sand on the walls of the hexagons, enhancing light emission. The light emitted from these hexagons, with a certain height, is more efficient compared to a larger flat panel with the same surface area and phosphorescent sand concentration per unit area. This design ensures that the panel remains compact, lightweight, and easy to manage in the confined spaces of latrine facilities, while maximizing the brightness and durability of the lighting solution.

In addition, the geometry of our panel was inspired by honeycomb structures, sandwich panels commonly used in architectural cladding, aerospace, and civil engineering applications. Honeycomb sandwich panels feature a honeycomb core adhesively bonded to front and back face sheets, offering high strength-to-weight ratio, rigidity, dimensional stability, and resistance to crushing and fatigue. In our design, we eliminated the face sheet and adhesive to create a monolithic form. This design choice allows the panel to be manufactured as a single, seamless unit, enhancing its structural integrity, improving durability, and simplifying the manufacturing process. Our unique design and prototypes are developed for mass production, ideally using vacuum thermoforming of acrylic or polycarbonate pellets mixed and extruded with strontium aluminate.

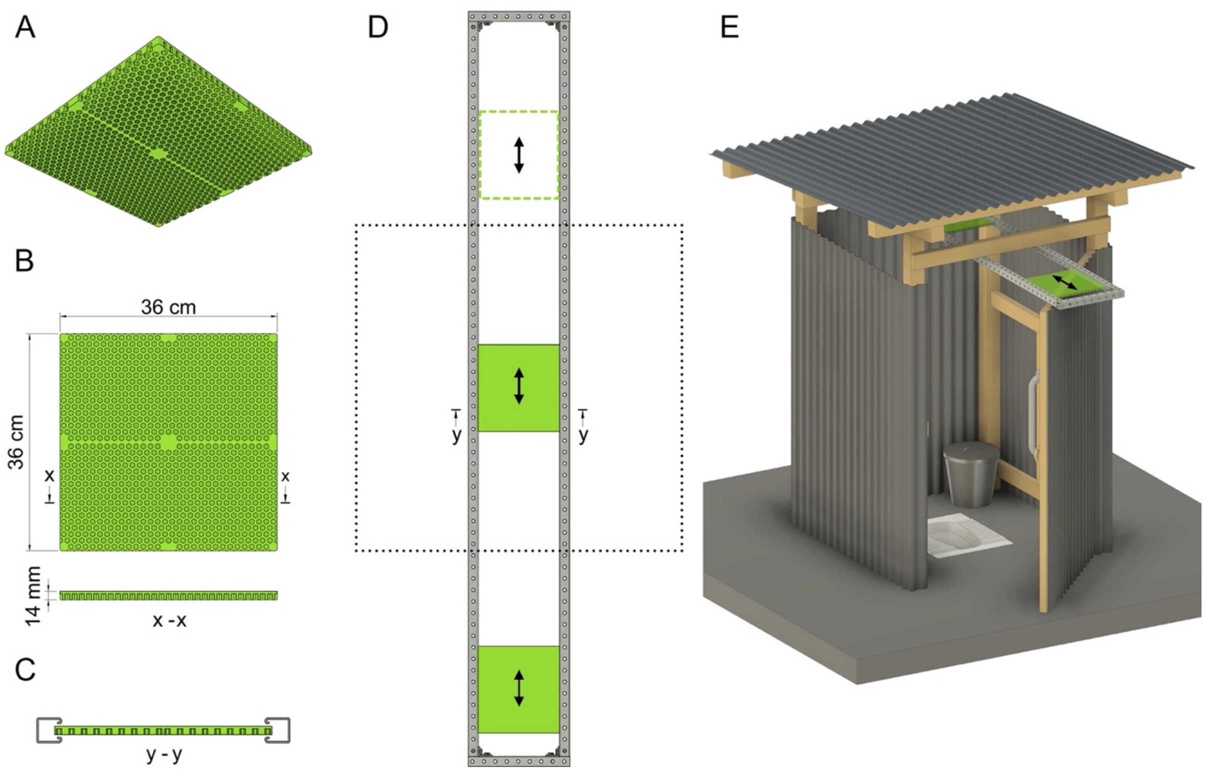

Fig. 1 | Design Overview and Integration with Latrine Structure
A: Provides a 3D view of the phosphorescent panel, highlighting the honeycomb surface.
B: Shows plan and section views of the panel with dimensions (36 cm x 36 cm and 14 mm thick).
C: Section through an example design illustrating the panel in the slot, allowing for sliding movement inside or outside the latrine for charging and illuminating different areas.
D: Illustrates a plan for the housing mechanism, comprised of metal framing struts to secure the panel. The dotted square represents the footprint of the latrine. Green squares indicate the movable panels, which can slide in the directions indicated by the arrows along the length of the theft-resistant frame structure. The authorities can secure the insertion, removal, and positioning of the panel by blocking the round holes of the frame with an ordinary padlock.
E: Displays the latrine with the housing mechanism for the phosphorescent panel (shown in green) attached to the latrine structure.

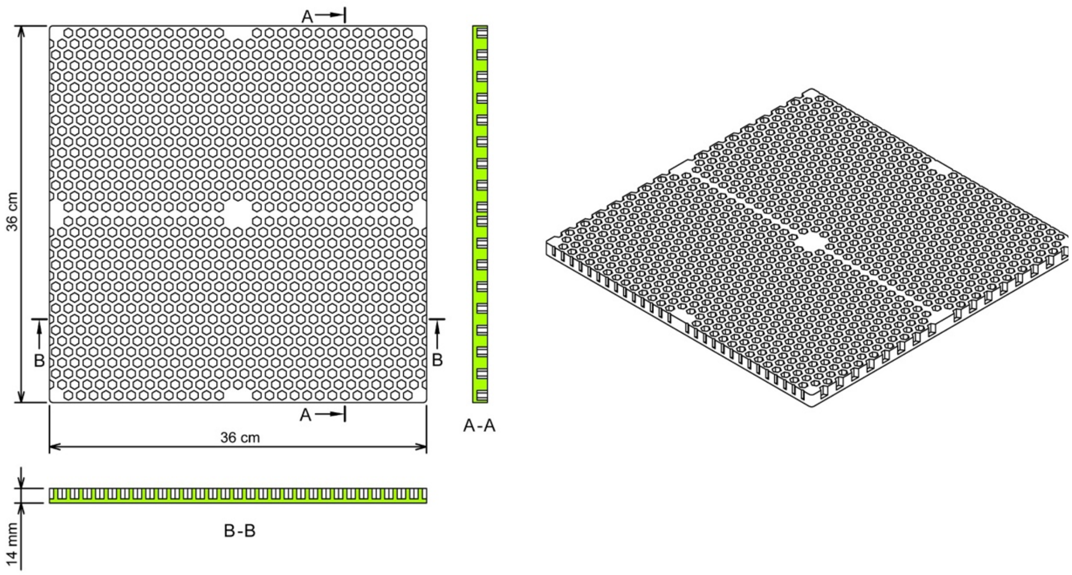

Fig. 2 | Schematics and 3D Representation of the Phosphorescent Panel
The drawing shows the top view and cross-sections (in green) with the phosphorescent material embedded in the panel structure (left), and a 3D view of the panel (right). The honeycomb patterning is clearly depicted in the schematic.

Rationale and Logic

Our honeycomb patterned panel design was aimed at maximizing light emission, minimizing weight, and enhancing durability. Based on the solution requirements and the specific needs to be addressed, we concluded that a phosphorescent panel of an effective geometry, decent size and thickness is the most feasible, versatile and cost-effective phosphorescent technology solution for latrine illumination. A panel that can be retrofitted inside a latrine can be easily mass produced with thermoforming or injection molding can also be secured in various methods. We designed our prototype to maximize the effectiveness of this type of solution, substantially improve useability with reduced costs. The honeycomb shape was selected for the extrusion geometry for multiple reasons. First, a honeycomb covers the most area with the least perimeter, allowing for the storage of more phosphorescent material in a larger volume while minimizing construction costs. This enhances portability and provides space for securing the prototype in latrines, reducing the risk of theft due to its compact yet sufficient size.

Second, the ability of hexagons to tile with no gaps or overlaps allows the embedded phosphorescent material to absorb and emit light with maximum efficiency. This allows increased uniformity, optimized space utilization, and reduced waste, thus simplifying manufacturing and reducing cost. Our design unit of hexagons is shown in Fig. 3 with dimensions that were optimized for maximum light emission and phosphorescent material packing. The honeycomb pattern also makes the panel durable and prevents bending in repeated cycles of heat if extruded from suitable plastics such as plexiglass, acrylic or polycarbonate.

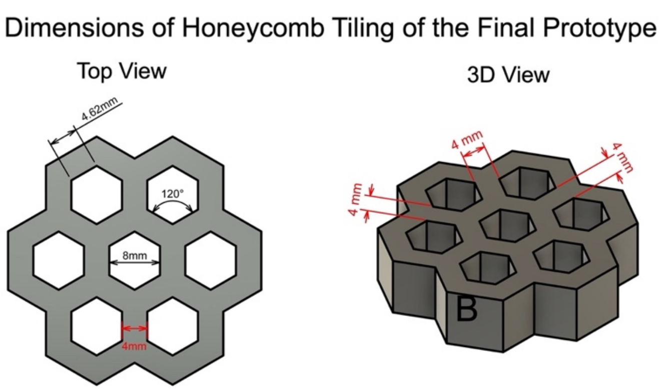

Fig. 3 | Optimal Dimensions of the Hexagonal Honeycomb Panel. A hexagonal honeycomb structure provides the most area with the least perimeter, enclosing more space using the same amount of material or less. A panel with 4 mm thick walls is determined to be the optimal thickness for illumination by embedded strontium aluminate

Space Efficiency and Structural Strength
In addition to space efficiency, hexagons stack in an offset arrangement with six short walls around each unit, providing high compression strength and excellent heat dissipation. This prevents damage from day and night cycles. The natural world, including beehives and wasp nests, utilizes hexagonal cells for these benefits. Hexagons, being the highest-sided polygons that fit together, minimize material usage and optimize space for light emission.

Material Efficiency and Cost Reduction
The honeycomb geometry reduces the quantity of material needed, both in the plastic used to embed the phosphorescent sand and in the amount required for sufficient light absorption and emission. This results in minimal weight and material costs, making the design suitable for low-cost production methods like thermoforming.

Durability and Resistance
Honeycomb panels exhibit minimal density while maintaining high tension strength and out-of-plane compression strength, thus enhancing their durability. The design ensures high strength-to-weight ratios, resistance to environmental damage, and the ability to withstand high temperatures and moisture absorption.

Conclusion
Our hexagonal honeycomb panels provide exceptional strength, space efficiency, and cost benefits. These features make them ideal for use in refugee camps, where efficient, durable, and cost-effective lighting solutions are critical. The design is easily machinable and formable, ensuring practical implementation and significant cost savings.

Benefits and Use Case for Phosphorescent Panel with Honeycomb Design Compared to Flat Panels

The designed panel offers significant advantages in terms of material usage, strength, light emission, security, casing, latrine installation, and production methods. Our phosphorescent panel features a hexagonal honeycomb structure with 4 mm thick walls, optimizing both material usage and performance. The 4 mm thickness was found to be the optimal balance between durability and light diffusion, as anything thicker did not significantly enhance the phosphorescent effect due to internal diffraction of the embedded material (see Fig. 6). Additionally, a thicker panel would increase production costs without proportional benefits. We compared the design with a flat panel based on the amount of light emitted from the surface and the density of the strontium aluminate in plastic (Fig. 4A, B).

If we were to create a flat panel with the same surface area of 5,548 cm^2 and 4 mm thickness, it would measure approximately 52.285 cm x 52.285 cm. This flat panel would require more phosphorescent material to achieve the same level of illumination, making it less efficient (Fig. 4C). Moreover, the thin plastic of a flat panel would not withstand daily sunlight and dark cycles, leading to faster degradation. **Our rationale was proven during the testing phase. When the prototype was hung from the ceiling of a completely dark room with the honeycomb side facing the floor and the flat side facing the ceiling (note that the ceiling is much closer to the prototype than the floor), the results showed that even though the flat side was much closer to the ceiling, the light emitted from the honeycomb side facing down was approximately an order of magnitude brighter (Fig. 4D). This proved that the honeycomb design has very high illumination efficiency.**

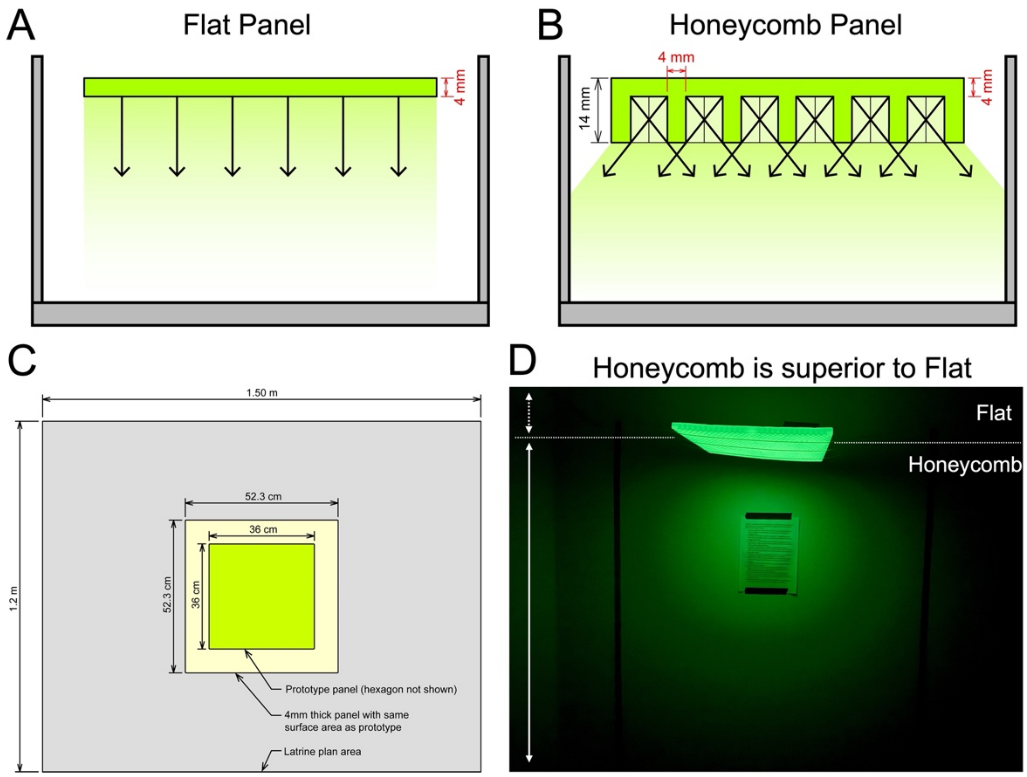

Fig. 4 | Comparison of Honeycomb and Flat Panels for Latrine Fitting
A. Phosphorescent flat panel with 4 mm thickness emitting light.
B. A panel with similar dimensions and a honeycomb pattern emitting light from the walls.
C. Comparison of a honeycomb-patterned panel and a flat panel with equal surface area embedded with the same area of strontium aluminate.
D. A photo of the prototype in a dark room, hung from the ceiling, showing that the honeycomb side of the panel emits an order of magnitude more light than the flat panel. Note the distance of the panel to the ceiling (dashed arrow) vs the honeycomb side facing the floor (arrows). The dashed line shows the sides facing the ceiling or floor.

Housing Mechanism and Theft Resistance

Securing a phosphorescent light panel in a refugee camp setting, particularly within latrine facilities, requires careful consideration of both functionality and security. The panel needs to charge during the day and safely illuminate the space at night without being at risk of tampering or theft. Our housing mechanism solution ensures both theft resistance and easy access for recharging.

We propose two primary variations for securing the panel, both utilizing the Unistrut metal framing system, commonly used for supporting and securing solar panels. These systems are adaptable, use common building materials that do not require specialized tools or welding, and can be easily implemented in the field. Additionally, they can accommodate multiple lighting solutions, such as the proposed phosphorescent panels or solar panels with NiMH batteries and LED lights, which are low-cost and commonly used for garden or stair illumination.

The first variation involves a Unistrut metal frame secured to the latrine structure with tamperproof fasteners. The frame extends beyond the latrine footprint (Fig. 1D,E), with struts oriented to create a slot in which the panel sits and can be repositioned along the frame while remaining secured (Fig. 1C,D). This design allows the panel to be easily slid out of the latrine for charging in the sun and slid back inside for illumination. It provides adjustable lighting levels and allows latrine users to move the panel without staff assistance.

The second, more basic variation, has the frame contained entirely within the footprint of the latrine with the panel secured in place. One side of the frame is hinged and secured with a lock, allowing the panel to be removed for recharging. This design necessitates daily labor by camp staff to unlock, remove, recharge, and reinstall the panel. Schematics for this variation can be provided upon request.

The Unistrut frame materials include slotted metal framing struts made from modular steel with perforated box section channels, providing high torsional resistance and lightweight properties. This framing system allows for multidirectional connections without drilling or welding. The framing components can be connected and attached to the latrine with tamperproof hardware, which is recommended to deter theft and tampering. This hardware is not easily removed without specialized tools, making it difficult for potential thieves to tamper with or remove the panel. An optional trolley track system can enhance the sliding mechanism for the panel in the first variation. **In any embodiment of metal framing system, the insertion, removal, and positioning of the panel can be secured by blocking the round holes with an ordinary padlock installed by the authorities.**

An alternative to the metal framing system is direct attachment to the roof. This involves cutting a hole in the roof where the panel will be installed and securing it with mounting brackets and tamperproof fasteners. The panel is centered over the hole and sealed around the edges with waterproof sealant to prevent leaks. This method provides a fixed installation that allows charging of the phosphorescent panels in place and is not easily accessible for tampering or theft. Although this approach does not introduce direct sunlight into the latrine, the concentration of the phosphorescent material embedded in the plastic will provide illumination from the phosphorescent material itself during daylight hours. This option presents risks as insects will likely be attracted to the panel, which is translucent and will emit illumination as it charges during the day.

Our proposed solution ensures that the phosphorescent panels are securely mounted, theft-resistant, and accessible for regular recharging, providing a practical lighting solution for the latrines.

Detailed Information of the Phosphorescent Material

Material Composition, Properties, and Source of the Phosphorescent Material

The choice of phosphorescent material in this solution was 500μm particle size phosphorescent sand from TechnoGlow, Inc (Fig. 5A). The phosphorescent material is Strontium Aluminate doped with Europium and Dysprosium, uncoated, with reported heat resistance up to 1100°C, suitable for thermoforming and injection molding. TechnoGlow products were reported by the vendor as the brightest and longest-lasting commercially available phosphorescent compositions in the US and worldwide. The 500μm particle size sand is the largest particle size commercially available and is the brightest and longest-lasting reported by the vendor. We also tested smaller particle sizes of 50μm (Kryptobryte) and large phosphorescent flakes (from eBay), but they were not nearly as effective as the luminophores material from TechnoGlow.

Reported Brightness for the Material:
1 Minute: 6080 mcd/m²
10 Minutes: 981 mcd/m²
60 Minutes: 220 mcd/m² respectively

First, we examined the properties, particle size, and confirmation of the properties as described in this section. Additionally, the luminosity was tested with varying amounts of sand in prototype resin casts with a commercial lux meter and advanced high dynamic rate TSL2591 sensor programmed for time-lapse studies.

Microscopic Examination

Upon receiving the phosphorescent sand, we evaluated the particle size and morphology under high magnification embedded in epoxy resin with varying amounts of sand (Fig. 5B). Microscope slides with varying concentrations of phosphorescent sand in resin, representing a 2D packing, were analyzed under a microscope. Particle size was determined using a micron scale ruler, with a 500μm x 500μm grid (Fig. 5C). The images were also taken in the dark after charging with UV light to better evaluate glow properties at high magnification (Fig. 5D). The results indicated the reported particle size and properties were accurate. For quantitative analysis, images taken from the slides were further analyzed, and the particle size distribution was determined by counting particles and measuring rough diameters using image analysis tools with ImageJ software. The results were plotted (Fig. 5E). This analysis helped determine the particle size distribution and density within a resin matrix such as epoxy or acrylate.

From this 2D analysis, it was projected that in a 3D packing, a maximum of 20-30% sand to resin ratio is optimal, as higher concentrations did not appear to provide better dispersion and packing. The results also confirmed that the reported particle size was accurate, with the median particle size being 534μm and a standard error of the mean (SEM) of 11.2 (Fig. 5F). The spread of the particle size distribution by range and percentiles showed that this material was highly suitable as the phosphorescent material for our prototype. The particle size distribution and density analysis confirmed that the average particle size of the phosphorescent sand luminophore is indeed 500μm. The optimal packing density was determined to be approximately 30% by weight of phosphorescent sand to resin, with higher concentrations leading to decreased light dispersion. This is due to insufficient gaps between particles, which are crucial for effective light penetration and emission. The optimal concentration for balancing cost, light absorption, and emission was established between 200-300mg of sand per gram of resin.

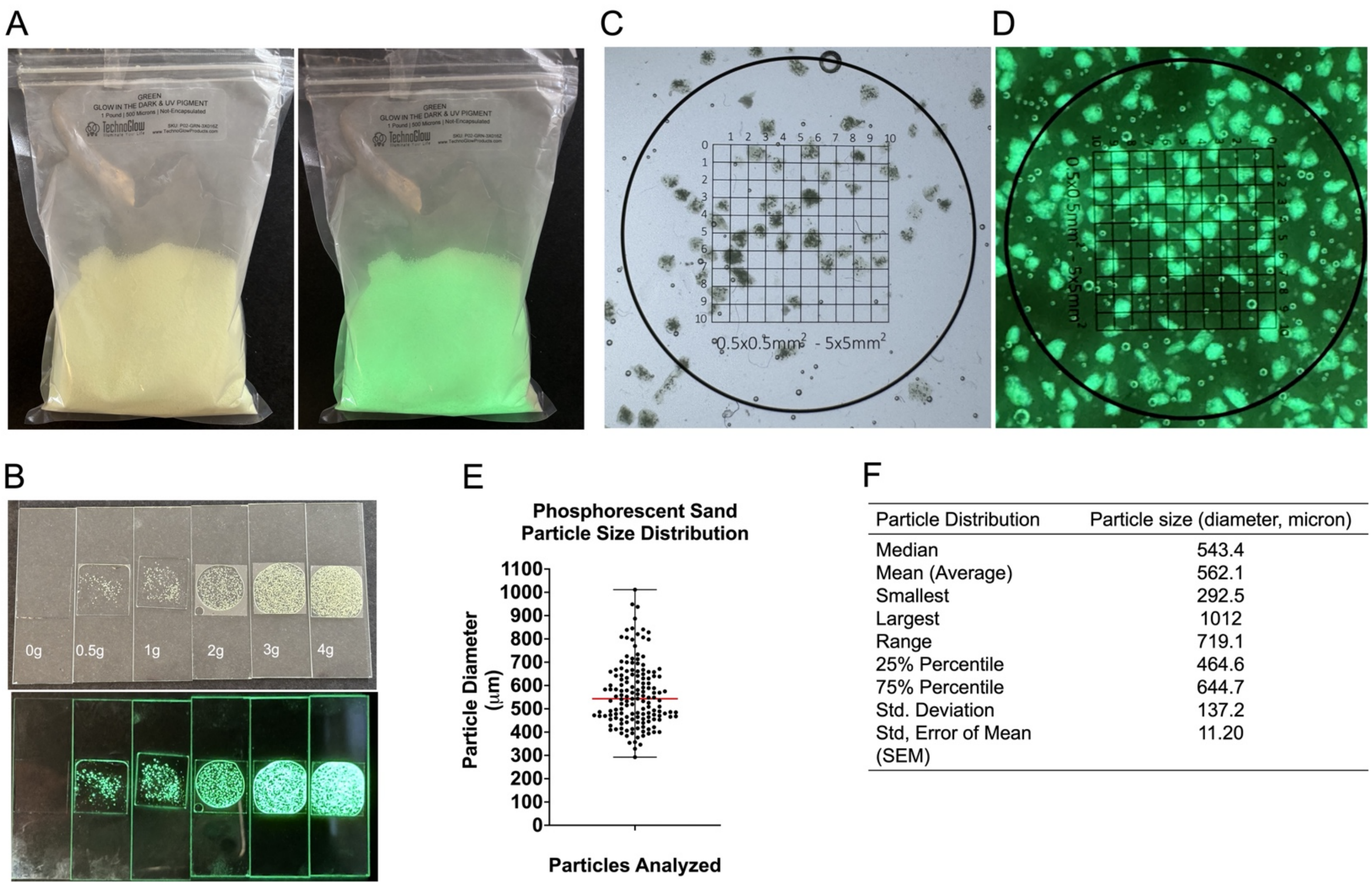

Particle Distribution	Particle size (diameter, micron)
Median	543.4
Mean (Average)	562.1
Smallest	292.5
Largest	1012
Range	719.1
25% Percentile	464.6
75% Percentile	644.7
Std. Deviation	137.2
Std, Error of Mean (SEM)	11.20

Fig. 5 | Evaluation and Properties of Phosphorescent Sand Embedded in Epoxy Resin
A. Phosphorescent sand (500µm) purchased from TechnoGlow, Inc. The sand (right) is exposed to UV light to observe the glow (left).
B. Varying amounts of phosphorescent sand (500µm) mixed with 10ml epoxy resin and mounted on glass slides.
C. Microscopic evaluation of phosphorescent particles measured with a 0.5mm x 0.5mm grid scale over the slides for the seeker's evaluation.
D. Similar image captured after UV light illumination for better visualization under illumination conditions.
E. Particle size diameter analysis from the microscope slides with 2g of sand per 10ml resin (optimum dispersal for measurement was 2g). Note: All particles analyzed were plotted. Red line: Median, Black lines: Range (Minimum-Maximum) sized particles.
F. Descriptive statistics of the particles and their distribution based on size (diameter).

Prototype Construction with Epoxy Resin Mixed with Phosphorescent Material

To build a plastic panel prototype representing the future mass-produced phosphorescent panels, we tested UV-curable acrylic resins and epoxy resin. Epoxy resin gave the best results in terms of clarity and effective mixing and dispersion. Therefore, the prototypes were cast in epoxy resin. It is important to note that this method is most feasible for demonstrating the design at the prototyping stage. For actual production, much lower-cost methods such as thermoforming using acrylate or polycarbonate are preferable. These materials will allow for faster production, providing simultaneous mixing and casting. Both acrylate and polycarbonate have excellent material properties, making them suitable for phosphorescent panels that meet solution requirements. The process of casting with epoxy resin was straightforward. By mixing epoxy and catalyst in equal volumes, the reaction started. After several tests, we determined that the best time to pour the phosphorescent sand-mixed resin was at 55 minutes. Adding the sand to the resin 10 minutes before this point and mixing rigorously produced a well-dispersed panel prototype.

Determining Phosphorescent Sand Amount and Thickness of Panel Walls

The analysis focused on determining the maximum effective thickness of resin that would optimize light emission from the panel, with the goal of determining the thickness of the honeycomb hexagonal tile walls. The rationale behind this analysis was to find the optimum thickness where the plastic can contain the maximum amount of phosphorescent sand while emitting the maximum amount of light without causing excessive light bounce and absorption by the plastic resin. It was found that thicknesses above 4mm did not provide additional benefits in terms of light emission efficiency. Therefore, a resin thickness of 4mm was selected for optimal performance in the final product design.

Epoxy Resin Thickness and Illumination Efficiency

First, ladder-like samples with incremental thicknesses (2-6mm) were created using 3D printing technology (Fig. 6A, left). Silicone molds from 3D-printed ladder-like samples were cast, and using these molds, epoxy resins were prepared with and without phosphorescent sand (Fig. 6A). These shapes were then used to make silicone molds for casting the epoxy resin mixed with increasing concentrations of phosphorescent sand (1-5 grams per 10 grams of resin). After UV exposure to direct sunlight to charge the phosphorescent materials, the casts were photographed under dark conditions in a black box. Each sample was isolated by black cardboard barriers to ensure there was no light interference, allowing for precise analysis.

Image Analysis

The photograph of these epoxy resin samples, embedded with varying concentrations of phosphorescent sand and set in silicone molds of incremental thicknesses (2-6mm), were taken in complete darkness in a black box. ImageJ software was used to analyze these images. A consistent region of interest (ROI) was chosen for each sample in rectangles of the same size across all thicknesses. The light intensity emitted from each sample was quantified in arbitrary units, which were compared to a control sample of clear epoxy cast with no phosphorescent material, giving a zero arbitrary unit value for clear epoxy. This comparison provided a detailed assessment of light emission efficacy across different sand concentrations and resin thicknesses

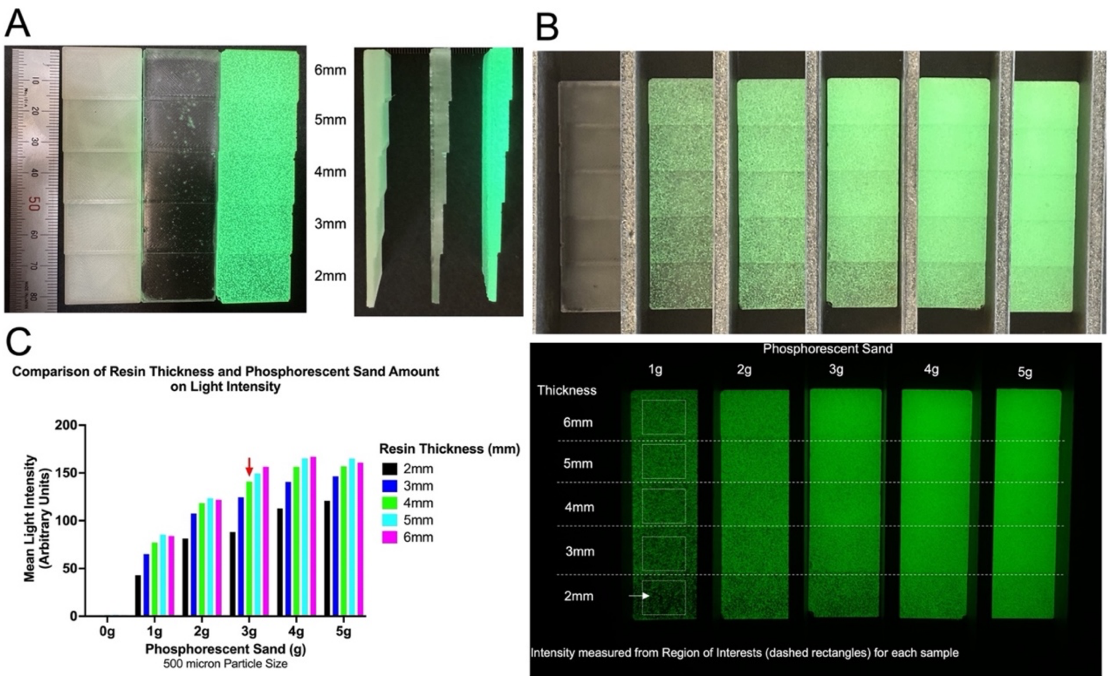

Fig. 6 | Effects of Resin Thickness and Phosphorescent Sand Concentration on Light Intensity
A. Ladder-shaped 3D printed sheets with incremental thickness (2mm to 6mm) were used to cast corresponding epoxy samples.
B. Epoxy resin casts mixed with 1g to 5g of phosphorescent sand in light and dark conditions. Photos taken in the dark after UV exposure were analyzed. The light intensity inside a rectangular box region of interest for different thickness of samples with increasing amounts of phosphorescent material was measured with ImageJ software.
C. Effects of resin thickness and phosphorescent sand were shown in a bar plot. Light intensity is measured in arbitrary units.

Prototype Testing Methods and Explicit Tests

The prototypes and the design iterations were tested using lux meters and high sensitivity light sensors programmed for time-lapse measurements as described in the methods section. The measurements were done inside a box designed for exact lux/lumen and millicandela measurements. Videos and photos captured for demonstration were done in a completely dark room with a setup simulating the dimensions of the latrines at zero hour and ten hours. Video and photo time stamping were done accordingly (Video 1,2). Time-lapse and lux measurements were performed with immediate measurements representing full charge, measurement after 1 minute, as described in TechnoGlow's product sheet, and at 10-minute intervals for 12 hours, automatically logged into an SD card. Calibrated lux data and mcd/m² were plotted using GraphPad.

Methods Used to Test the Phosphorescent Materials, Including Light Emission Tests

The effectiveness of the panels was tested under various lighting conditions, including direct sunlight and cloudy days, to assess their luminescent properties after 3 hours of sun exposure. These tests were conducted inside a measurement box designed to accurately gauge lux, lumen, and millicandela values at 0, 6, and 12 hours. Additionally, time-lapse studies were performed to monitor the light output over 12 hours with 1-minute intervals using a TSL2591 light sensor integrated with an ESP32 microcontroller, calibrated against a commercial lux meter (Dr. Meter).

Measurement of Lux, Lumen, and mcd/m²

To accurately measure the lux, lumen, and millicandela values of phosphorescent panel prototypes, a specialized measurement box was constructed (Fig. 7A). The box was specifically designed with dimensions that ensure 1 lux equals 1 lumen. The distance of the sensor facing the phosphorescent panel was exactly 28.2 cm, enabling direct conversion to millicandela across its 0.99 square meter interior, simulating the surface area of a light sphere reaching 1 square meter. This configuration allows for straightforward calculation of mcd/m²

Measurement Box Configuration

Dimensions: 40 x 40 x 28.2 cm (L x W x H). The height of the box (28.2 cm) is tailored to equate 1 lux to 1 lumen at this measurement distance, which simplifies the calculation of millicandela considering a 360-degree radiation angle of a phosphorescent panel emitting light in the entire surface area facing the sensors. This is facilitated by the box's white-painted interior, which enhances total internal reflection. Sensors are mounted at the top of the box, while the light-emitting panels are positioned at the base (Fig. 7A,D).

The lux levels were primarily measured using a commercial lux meter (Fig. 7B) and the TSL2591 sensor due to its superior sensitivity, dynamic range, and capabilities. We ensured that the light box is completely dark and properly sealed (Fig. 7C) The sensor is connected to a microcontroller (Fig. 7E,F). The readings taken at 0, 6, and 12 hours post-exposure, as stipulated in the challenge description as well as time-lapse data logging were done with this setup. This measurement rig allowed us to measure in seconds, minutes, and hour intervals. Single-point measurements using the TSL2591 or Dr. Meter LX1330B lux meter were complemented by continuous monitoring using the high-dynamic-range TSL2591 sensor, which was programmed to record lux and light intensity every ten minutes over a 12-hour period. This advanced setup allowed the programmed sensor to record data on an SD card, either as single measurements or as a time-lapse of up to 24 hours with intervals ranging from 1 second to 60 minutes.

TSL2591 Advanced High Dynamic Range Digital Light Sensor

The TSL2591 is an advanced high dynamic range digital light sensor ideal for a wide range of measurements, from very bright (up to 68,000 lux) to very low light settings (Fig. 8A^{I},A$^{II.}$). It approximates human eye response and is more sensitive than many market alternatives, such as Dr. Meter, which has a limit of 0.1 lux. Measurements with different time intervals and durations tested the TSL2591's capabilities, including sensor gain and integration time from low, medium, high, and max settings. The sensor's sensitivity ranges from 168 microlux to 68000 lux, providing a sufficient range to measure phosphorescent panel luminosity over time.

The TSL2591 can measure the initial "superglow" properties of phosphorescent sand in second or minute intervals and its stabilized release over hours in very low light conditions. It supports the use of multiple sensor setups simultaneously for distinct time intervals and redundancy in time-lapse studies. Compared to Dr. Meter, this sensor not only has superior capabilities but also greater flexibility. Since commercial lux meters such as Dr. Meter or similar equipment are used ubiquitously for lux measurements in various settings, we converted TSL2591 readings to the Dr. Meter corresponding format.

Luminance Measurements with Advanced Time-Lapse Using TSL2591 High Dynamic Range Lux Sensor

We programmed an ESP32 microcontroller to control the TSL2591 sensor with sensitivity set at HIGH and integration time set at 300ms (Fig. 8B). This dual measurement approach allowed for the accurate plotting of both real-time and endpoint values. The measurements from the lux meter and TSL2591 were used to plot the results accurately. The box was specifically designed with dimensions that ensure 1 lux equals 1 lumen, enabling direct conversion to millicandela across its 0.99 square meter interior, simulating the surface area of a light sphere reaching 1 square meter. This configuration allows for straightforward calculation of millicandela.

Calibration

We calibrated TSL2591 results to Dr. Meter and provided the converted values of a commercial lux meter, where 11 lux from the TSL2591 equals 19.7 lux from Dr. Meter (Fig. 8D). We set the settings as close to Dr. Meter as possible for calibration. The sensor's advantage and the measurement setup lie in its time-lapse and data recording capabilities, from microseconds to hour intervals, and durations up to 24 hours, battery permitting. It was programmed using C++ with an ESP32-based microcontroller featuring data logging (SD card), a built-in display, extended battery life, and a keyboard.

The programming involved testing for sensor functionality, SD card, and microcontroller modes for various measurements (Fig. 8C). The Dr. Meter LX1330B lux meter and the TSL2591 sensor were tested using a green LED with a reported output of 1500 mcd/m², which is close to the measured value of 1588 mcd/m². When the TSL2591 sensor measured 11 lux, the lux meter measured 19.7 lux (Fig. 8D^{I}, D^{II}). We converted the TSL2591 lux values to corresponding lux values obtained by the Dr. Meter, as similar equipment is widely available and factory calibrated.

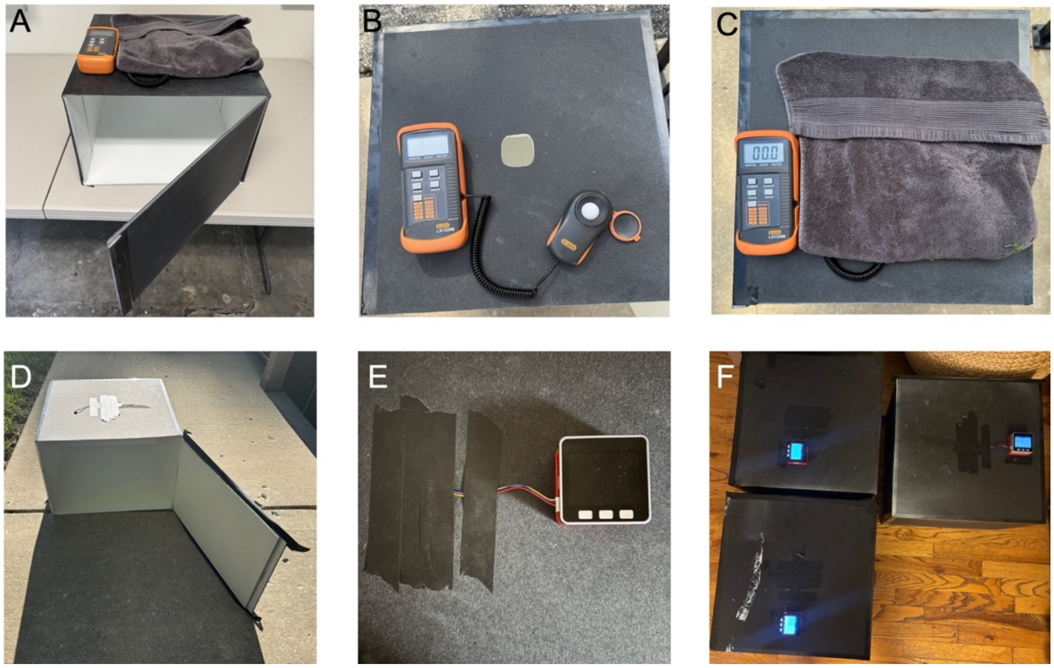

Fig. 7 | Measurement Box and Sensor Setup for Capturing Accurate Lux and Lumen Readings from Phosphorescent Panels in a Controlled Environment
A. 40cm x 40cm x 28.2cm completely sealed box for exact lux and lumen measurement from panels. The white interior captures maximum light for accurate lux measurement. The height of 28.2cm corresponds to a 1m² surface for accurate determination of millicandela. Note: 1 lux = 1 lumen with the box specifications.
B. The hole in the top middle of the box where a lux meter and lux sensor TSL2591, as well as an iPhone, can be secured.
C. Daylight, outside lux measurement inside the box, showing no light leaks into the box in the setup (lux meter shows a value of 0 lux).
D. Interior of the box and sealing method with black tape shown. The top of the box shows the TSL2591 sensor secured and sealed with black tape. The cable is for the I2C connection to the sensor with a microcontroller.
E. Overall TSL2591 setup for accurate time-lapse measurement. The computer is based on the ESP32 microcontroller with Wi-Fi, a real-time clock, and SD card data logging capacity. The computer can be programmed in situ to measure second to minute intervals and up to 24 hours duration.
F. Three measurement boxes with identical dimensions and three TSL2591 and computer setups for logging samples from three individual prototype panels. Due to the compact size, up to three TSL2591 sensors can be secured in a single box for more redundancy in accurate measurement of the final prototype.

Data Collection Protocol

Time-lapse measurements were taken over a 12-hour period, capturing data every minute using the TSL2591 sensor controlled by an ESP32 board. This detailed tracking was essential to evaluate the light decay profile of the phosphorescent panels. Lux measurements were specifically recorded at intervals of 0, 6, and 12 hours post-initial light exposure to assess the persistence of luminescence using a Dr. Meter lux meter. The results were analyzed and plotted using Prism Software. The table for initial and 1-minute lux/lumen and millicandela/m² measurements was provided for all the prototype iterations in order to compare the surface area and phosphorescent sand amount on luminance and also to evaluate the measurements reported by TechnoGlow datasheet.

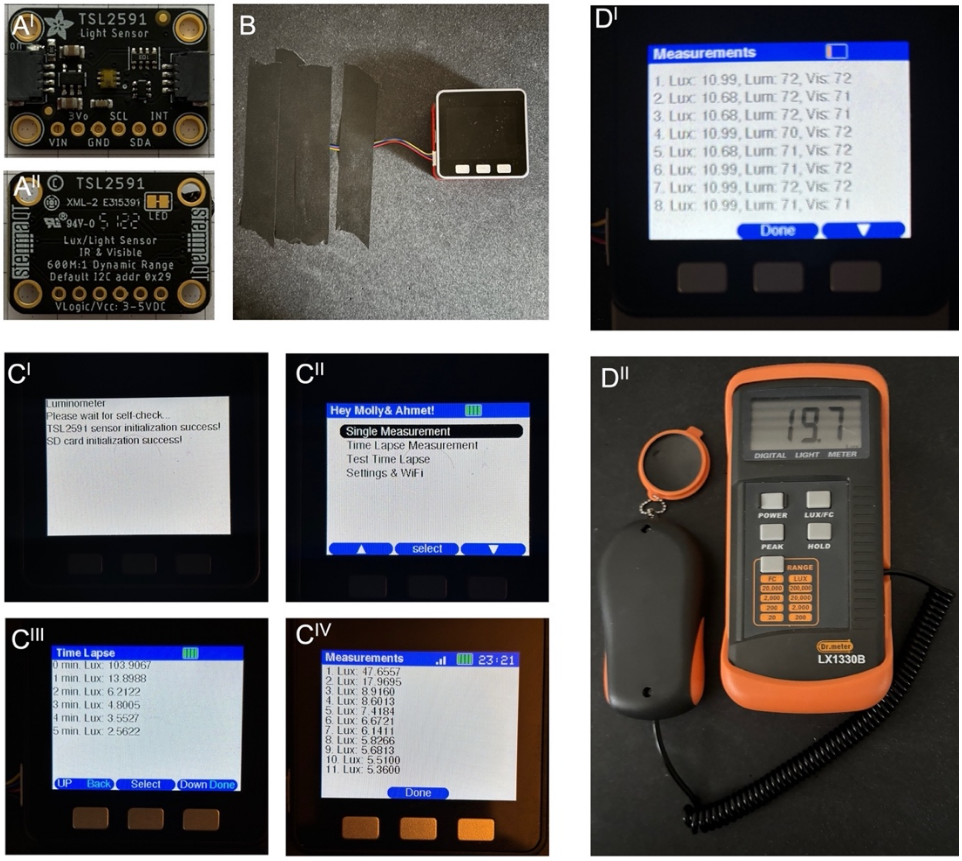

Fig. 8 | A Detailed Setup and Methodology for Measuring the Light Output of Phosphorescent Panels Using a High Dynamic Range Lux Sensor and ESP32 Microcontroller

A. TSL2591 high dynamic range lux sensor (168 µlux to 600,000 lux range).
B. TSL2591 secured to the box and connected to the computer.
C^{I}. Programming and self-check proof of the ESP32 microcontroller for lux measurement, indicating the sensor is recognized and working properly, and the SD card is ready for data logging.
C^{II}. User interface of the program coded in C++ language, showing measurement modes and settings, and Wi-Fi capability for remote sensing.
C^{III}. Time-lapse example from one of the panels for 1-minute intervals. Lux sensor and data logging setup for precise light measurements.
C^{IV}. Single measurement mode, where each sample can be measured and logged, making it easier to measure multiple samples, such as 1 minute after sun exposure to compare TechnoGlow reported values.
D^{I} and D^{II}. Corresponding lux measurement from Dr. Meter. The values are used to calibrate the TSL2591. A 19.7 lux reading from Dr. Meter corresponds to 11 lux in the TSL2591 in high sensitivity setting with a 300 ms integration time (for very low light measurement).

Development and Testing of Phosphorescent Panel Prototype

Initial Design and Exploration

The prototype development began with the design of honeycomb-shaped panels measuring 8 cm x 8 cm, which were 3D printed using off-white PLA filaments that contained a low concentration (estimated to be not more than 2%) of phosphorescent luminophore. The cost-effective filament, although much lower concentration of phosphorescent sand, priced at $20 per kg for hobbyists printing two 36 cm x 36 cm panels, which was promising for the similar phosphorescent sand embedded polymers as a desired solution that can be mass-produced. This initial stage demonstrated the feasibility of producing larger panels infused with a higher concentration of phosphorescent materials through injection molding. Epoxy resin and phosphorescent sand (500µm) purchased from commercial vendors were used to develop, optimize, and test the prototype's properties and output.

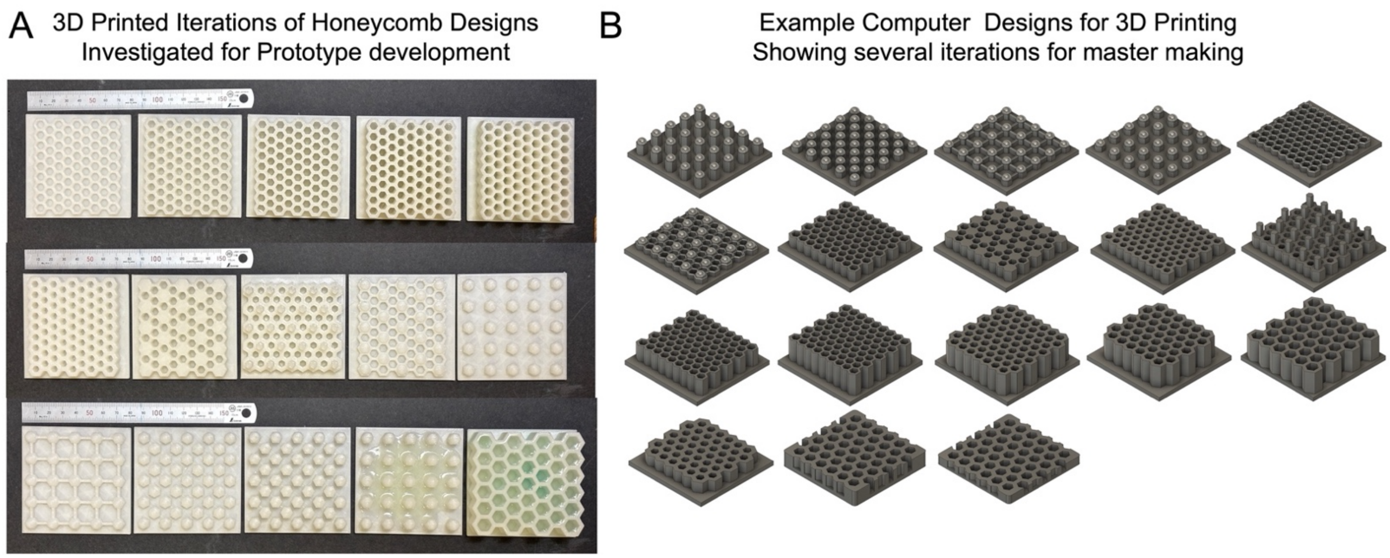

Fig 9. | 3D printed Honeycomb Design Iterations for mold making (8cm x 8cm)
A. Initial 3D printed 8cmx8xm models with phosphorescent PLA filaments with various hexagonal tiling honeycomb structures to determine the optimum glow and surface area for the casts.
B. Final last three designs were utilized for further development of the prototype.

Silicone Molds and Epoxy Casting

Following the 3D printing phase, silicone molds were created from 3D prints as templates to cast epoxy resin mixed with phosphorescent sand (Fig. 10A-D). The epoxy resin mixing and time of pouring of the resin mixed with phosphorescent sand was determined. Different concentrations of the phosphorescent sand and honeycomb panels with varying sizes corresponding to a specific surface area/weight phosphorescent sand were experimented with across various dimensions of the resin.

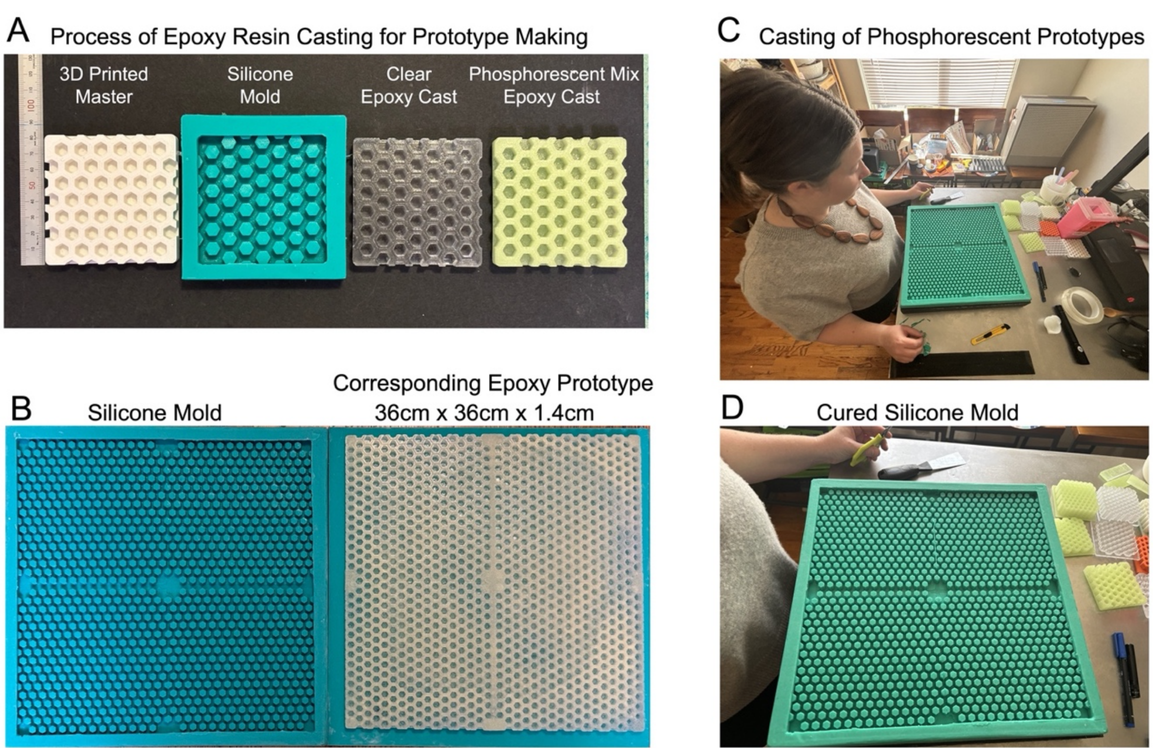

Fig. 10 | Process for Building Prototypes with Cast Epoxy Resin Embedded with Phosphorescent Sand
A. 3D printed models used as positives to create silicone molds for casting the prototypes.
B. Example of a silicone mold for Prototype 1.
C. Epoxy casting process using the final molds.
D. Closer examination of a mold created for Prototype 1.

Design Iterations for the prototype

Initial 3D printed 8 cm x 8 cm models using phosphorescent PLA resin with various hexagonal tiling honeycomb structures were used to determine the optimum glow and surface area for the casts. We proceeded to create silicone molds and cast the iteration of the designs with epoxy. The final three designs with honeycomb wall thickness and height were utilized for further development of the prototype with increased size per cast and varying phosphorescent sand amount (Fig. 11A,B).

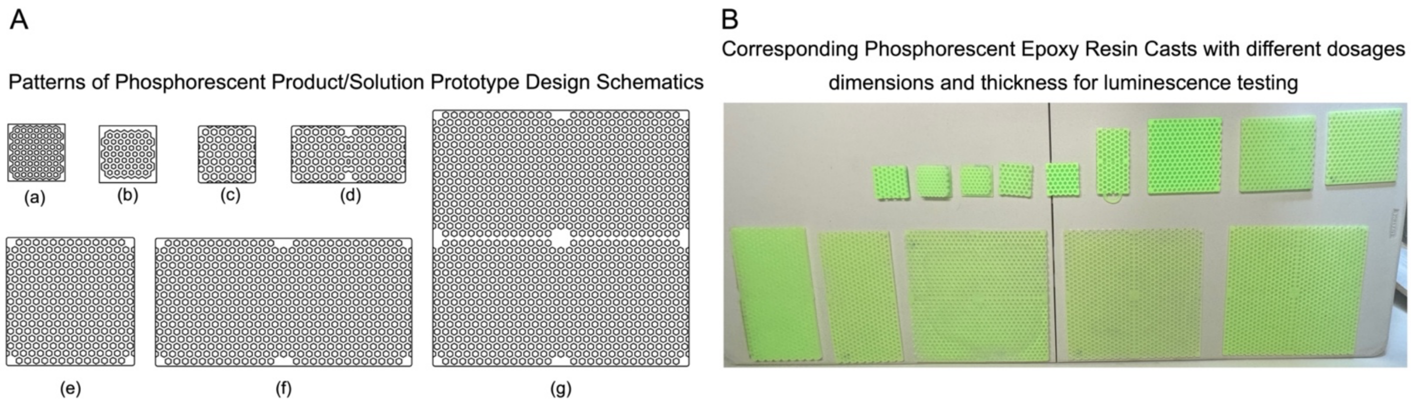

Fig. 11 | Final Prototype Iterations with Different Dimensions and Phosphorescent Sand Mix
A. Schematics of the prototypes designed, showing various iterations.
B. Corresponding epoxy resin casts of the prototypes with the phosphorescent sand embedded in epoxy.

<u>Prototype Dimensions and Performance Metrics</u>

The results of our prototype metrics, including dimensions, weight, surface area, amount of phosphorescent sand added, and lux and millicandela measurements, can be found in Table 1. This table provides a comprehensive overview of the properties and performance metrics of each prototype. From the table, we gathered essential insights for the phosphorescent panel.

A general metric for the effect of the percentage of phosphorescent sand on luminosity can be estimated from the table. Increasing the percentage of phosphorescent sand from 10% to 22% results in a 2.36-fold increase in luminosity, suggesting a linear relationship up to 30% as we determined with the epoxy casts with different concentrations. For a given dimension, the luminosity is proportional to the percentage of phosphorescent sand. Crucially, when the surface area of the panel is doubled, the luminosity increases fourfold, given the same percentage of phosphorescent sand. For example, Prototype P1 and a theoretical panel with double the surface area but the same percentage of phosphorescent sand would demonstrate this effect.

Table1 provides a detailed comparison of the physical and performance properties of each prototype, highlighting the effectiveness of different designs and materials used. Additionally, we included a one-minute time-lapse graph with one-second intervals to determine the initial superglow of the phosphorescent material and its luminosity.

Table 1 | Properties and Metrics of the Prototypes

Prototype	dimensions LxWxH (cm)	Surface Area (cm^2)	Volume (cm^3)	Weight (g)	Strontium Aluminate (g)	% Strontium g/Weight	Lux/ Lumen (initial)	Lux Lumen (1 min)	Luminance mcd/m^2 (initial)	Luminance mcd/m^2 (1 min)
P1	36 x 36 x 1.4	5549	1257	1825	400	22	470	60	37380	4771
P2	36 x 36 x 0.8	4358	703	1251	270	22	436	56	34670	4453
P3	36 x 36 x 0.8	4358	703	1004	100	10	185	48	14712	3817
P4	36 x 36 x 1.4	5549	1257	1513	150	10	190	24	15110	1906
P5	18 x 36 x 0.8	2208	351	487	87.5	18	146	28	11610	2227
P6	18 x 36 x 1.4	2826	428	870	90	10	198	19	15746	1511
P7	18 x 18 x 0.8	1116	156	247	60	24	107	28	8509	2267
P8	18 x 18 x 1.4	1430	321	429	75	17	125	14	9940	1113
P9	18 x 18 x 1.4	1430	321	480	90	19	169	15	1344	1192
P10	8 x 16 x 1.4	574	125	203	60	30	45	25	3579	1988
P11	8 x 8 x 1.4	295	63	94	15	16	29	9	2306	715
P12	8 x 8 x 1.4	295	63	78	6.7	9	33	6	2624	477
P13	8 x 8 x 1.4	265	63	81	11.8	15	31	3	2465	238
P14	8 x 8 x 2.4	486	57	116	15.7	14	28	4	2227	318

We further evaluated the luminosity performance of various prototypes of phosphorescent panels by measuring their light output over a 60-second time lapse, recorded at 1-second intervals (Fig. 12A, B). This rapid assessment of the "superglow" phase serves as a good metric for gauging the maximum light accumulation capability of each panel when fully charged by sunlight, especially for prototypes with varying particle size and composition. We concluded that the supercharge state is most affected by the percentage of phosphorescent material up to 30%, confirming the image analysis in Fig. 6C. The superglow decays rapidly within minutes, and within 1 hour the output decays to microlux levels (Fig. 12C, D).

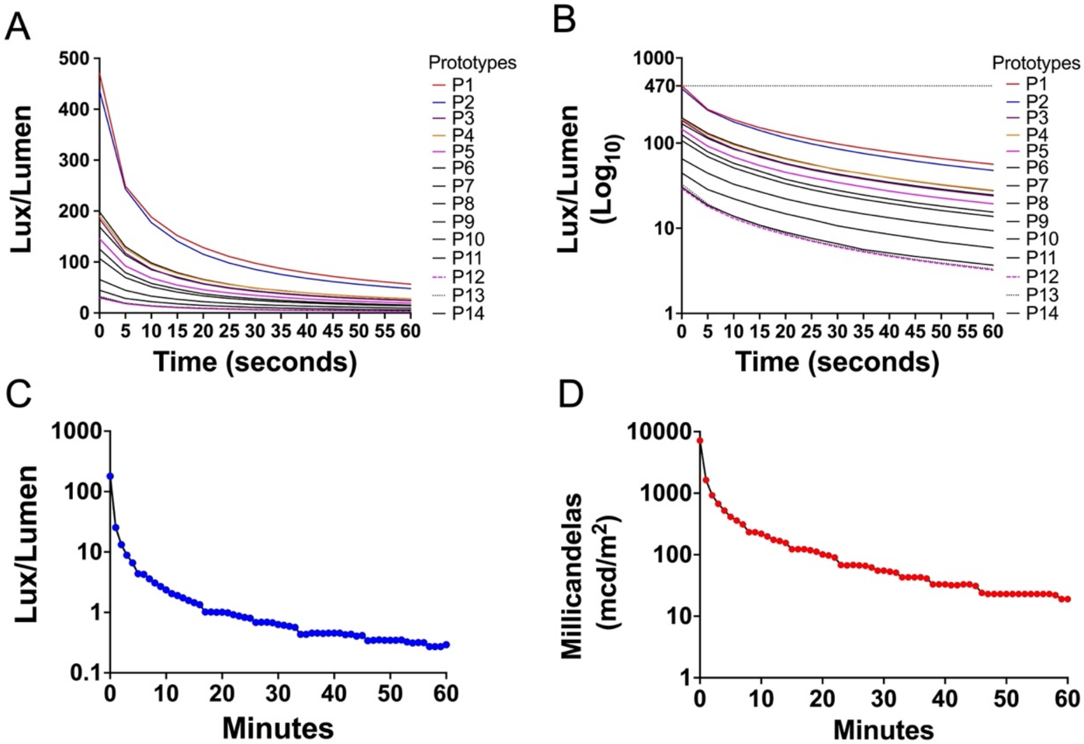

Fig. 12 | Time Lapse of Prototypes Testing "Superglow" Light Decay
A. Lux/Lumen measurements from the initial measurement to the 1-minute mark.
B. Semi-log plot of the measurements from the initial measurement to the 1-minute mark, providing a better spread between time-lapse data of the prototypes.

The test results from our final iteration, Prototype P1 under different cloud coverage indicated that after 4 hours, the light output decayed to sub-lux levels, but the light output remained stable at these lower levels for more than 12 hours (Fig. 13A, B). Therefore, the panels can be optimized for the percentage of phosphorescent sand and surface area to result in stable illuminance for up to 14 hours, with increased lux output. We did not see a clear effect of cloud coverage and charging time on the output during clear days and full cloud coverage. However, sensor readings were slightly lower on fully cloudy days during the initial superglow phase (data not shown), where we observed lower lux values. After the superglow phase, this effect was less pronounced. Sun exposure from either the back or the front of the panel fully charged it and did not affect the output.

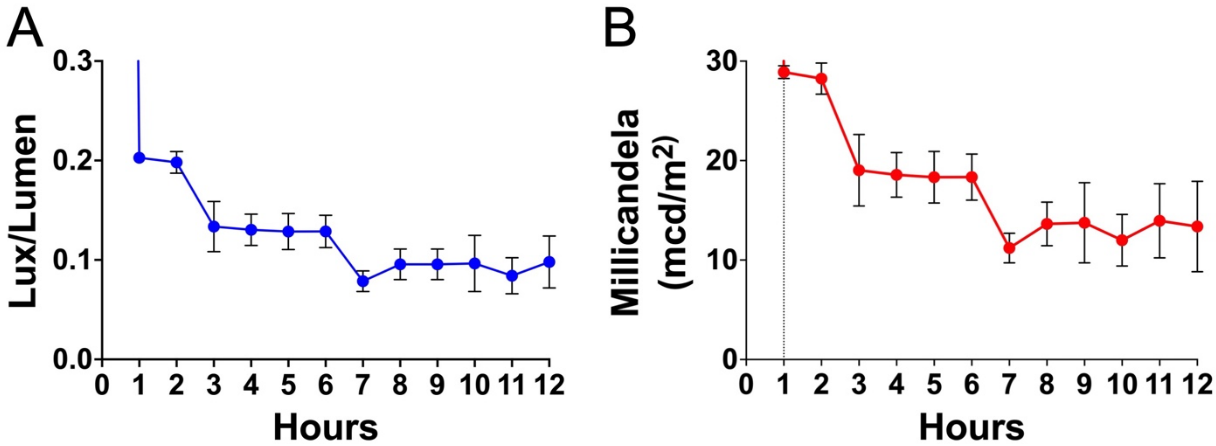

Fig. 13 | Time Lapse of the Prototype Over 12 Hours in 50% Cloud Conditions
A. Lux/Lumen measurements from the initial measurement over a 12-hour period.
B. Corresponding millicandela (mcd/m²) values over the same 12-hour period.

The panels can be charged for a minimum of 2 hours, with noon charging being faster due to more penetration of UV light. We observed the effects of charging due to the change in color of the panel from dark yellow to green even in daylight. The afternoon sun also has enough UV emission to charge the panels effectively.

Finally, to address the seeker's requirements, we filled the table they provided as shown in Table 2. We chose a day with 50% cloud coverage and charged the panel for 4 hours in partially cloudy conditions. Our measurement results were consistent on different days. The output was around 0.1-0.15 lumen in any condition, regardless of the charging duration. On this day, we charged for 4 hours before taking the panel to the measurement box for assessment.

Table 2| Test Results for Prototype 1 requested by IRC “the seeker”.

Prototype	**Date**	**RECHARGING** # of hours of light absorption (max 8 hours to full charge)	**RECHARGING** % cloud cover on this date	**OUTPUT** # of hours light emitted (min 12 hours)	**OUTPUT Hour 0** Lux Lumen *mcd/m²*	**OUTPUT Hour 6** Lux Lumen mcd/m²	**OUTPUT Hour 12** Lux Lumen mcd/m²
P1	05/20/24	4 hours	50%	12	301.6 301.4 *23984*	0.14 0.14 *11.3*	0.12 0.12 *9.3*

Simulated Use in Latrine Toilets, Videos and Results

The final testing phase simulated the real-world application by hanging the panel horizontally inside a dark room, mimicking the setup inside a latrine toilet. The panel was tested for its ability to illuminate text (A4 paper with 14.5 font size) taped to a wall. Video and photographic documentation captured the light output immediately after charging and after 10 hours, providing visual proof of the panel's efficacy (Video1). Due to the limitations and settings of the camera, the videos and time-lapse images did not accurately represent the level of illumination provided by the prototype that we observed in the room. A second 12-hour timelapse is provided with adjusted camera settings (Video 2).

Visibility

The simulated environment was a laundry room with dimensions of 3 m x 4.5 m and a height of 2.5 m. The room contained a table, a clothes rack, laundry machines, and a water heater. At the tested lux level, we could clearly see these pieces of equipment and individuals in the room. While we could not read 14.5 font text at the 10-hour mark, we could see the text on the page, and increasing the size of the panel beyond 36 cm x 36 cm could easily allow for reading. If reading is not essential, the lux levels were sufficient enough to operate. Additionally, the luminance level, while low, can be advantageous in preventing voyeurism and peeping from outside the latrines.

Adequacy for Reading

Based on typical lighting standards, a minimum of 0.5 to 1 lux is generally required for basic visibility in low-light conditions, while higher lux levels are recommended for reading tasks. For reading 14.5 font text comfortably, especially in a latrine, a light level closer to 1 lux would be more appropriate. Therefore, while the increased panel size and sand content improve the situation, it may still fall short for reading without further enhancements. To achieve optimal illumination for reading, combining phosphorescent panels with additional lighting solutions, such as low-power LEDs, might be necessary.

Increasing the panel dimensions and the percentage of phosphorescent sand significantly enhances luminosity, providing better visibility in dark conditions. For tasks such as reading, however, further light augmentation may be required to reach the desired illumination levels. A panel providing 0.45 lux might be sufficient for general visibility and navigating the latrine, and it is likely adequate for reading text in 14.5-point font. Increasing the panel to 50 cm x 50 cm with 30% phosphorescent sand content, yielding around 0.675 lux, moves closer to the lower threshold for reading and is fully adequate for latrine use.

Conclusion and Key Findings

Understanding the relationship between phosphorescent sand concentration and luminosity helps in the efficient use of materials, ensuring cost-effectiveness while maximizing performance.

Percentage of Phosphorescent Sand

Increasing the percentage of phosphorescent sand within a given volume of the panel leads to a linear increase in luminosity. For example, increasing the percentage of phosphorescent sand from 10% to 22% in a given volume results in approximately a 2.36-fold increase in initial luminosity. This indicates that the luminosity is roughly proportional to the percentage of phosphorescent sand used up to 30% material embedded in plastic.

Surface Area

Doubling the surface area of a panel, while maintaining the same percentage of phosphorescent sand per weight, results in a four-fold increase in luminosity. This effect highlights the importance of optimizing the surface area of the panels to maximize light output, especially in applications where space and efficiency are critical.

Stability of Luminosity

Our study also found that regardless of weather conditions, a sunlight-charged panel, such as our 36 cm x 36 cm prototype (P1), consistently decays to a stable luminosity of 0.1 to 0.15 lux after the initial superglow phase. This stable light output lasts for up to 12 hours. The consistent luminosity level indicates the panel's reliability in providing a minimal yet continuous light source throughout the night.

Visibility and Practical Use

In a completely dark room, this luminosity is sufficient to identify objects but not enough to read text in 14.5 font size at the 10-hour time mark. This indicates that while the panel improves visibility and safety in latrines, it may not provide adequate light for detailed tasks such as reading.

Impact of Increasing Dimensions and Scalability

By increasing the dimensions of the panel from 36 cm x 36 cm to 50 cm x 50 cm, and maintaining the same 20% phosphorescent sand content, the estimated luminosity increases to approximately 0.45 lux. This increase significantly enhances visibility. The demonstrated proportional relationship between surface area and luminosity supports the scalability of the design. Larger panels can be deployed in areas requiring higher illumination, while smaller panels can be used in more confined spaces, all while maintaining efficient light output. If the phosphorescent sand content is increased to 30%, the luminosity would increase proportionally. As exemplified earlier with 30% phosphorescent sand content, the estimated luminosity for the prototype panel will be 50 cm x 50 cm panel would be approximately 0.675 lux.

Our study highlights the critical parameters affecting the luminosity of phosphorescent panels: the percentage of phosphorescent sand, the surface area, the initial and long-duration output, charging time, and effects of cloud coverage. The designs and resulting data are crucial for understanding the fundamentals of generating a phosphorescent panel. By carefully adjusting these factors, we can significantly enhance the light output, making these panels a viable and efficient solution for improving illumination in refugee camp latrines. This approach not only enhances safety and visibility but also ensures the cost-effective use of materials, supporting the sustainability of the project.

Summary

In this submission, we conducted a thorough study on the design and testing of a prototype phosphorescent panel. We kindly request the International Rescue Committee (IRC) to review our design and thorough study on the properties of phosphorescent materials with decent particle size and premium quality as a baseline for evaluating plastic-embedded phosphorescent panels.

Our research found that the hexagonal panel design worked effectively based on our rationale. The phosphorescent panel exhibited a luminosity of 0.1-0.15 lux at the 12-hour endpoint, a value that remained consistent regardless of weather conditions, including clear skies, cloudy days, and fully overcast conditions if charged minimum 2 hours or more. We tested our prototype in a simulated environment and provided time-lapse videos and videos of the setup. As stated above, due to the limitations and settings of the camera, the videos and time-lapse images in Video 1 did not accurately represent the level of illumination provided by the prototype that we observed in the room. A second 12-hour timelapse is provided with adjusted camera settings (Video 2).

We also determined that the maximum effective phosphorescent material content that can be embedded in a plastic panel is 30%, beyond which there were no substantial benefits. Additionally, doubling the surface area of the panel increased the lux values fourfold, validating the scalability of our design. However, we faced limitations in our prototype dimensions, restricted to 36 cm x 36 cm with 20% doped strontium aluminate. Increasing the panel size and utilizing the maximum 30% phosphorescent material could provide the fulfilling performance.

Our prototype, produced using commercially sourced materials with significant markup due to hobbyist market dynamics in the US, cost $78. This cost is prohibitive, but we estimate that with a suitable business capable of mass production, the cost could be reduced to 10% of the prototype cost. We identified Zhejiang Minhui Luminous Technology Co., Ltd. in China as a potential manufacturer that can produce both the strontium aluminate phosphorescent material and the embedded panels efficiently.

For our study, we used phosphorescent sand costing $188/kg with a reported 6000 mcd/m² luminance. Another vendor offered a 3 mm particle size phosphorescent material with 9000 mcd/m² luminance at $110/kg. Due to budget and time constraints, we did not test this larger particle size but focused on studying the feasibility of panels embedded with strontium aluminate.

Our design clearly showed that the hexagonal design is efficient for illumination. The cost of epoxy resin was similarly high at $30 per gallon, but a business capable of mass production could significantly reduce this cost. We also tested phosphorescent flakes and powders, but they were not as bright or long-lasting as the phosphorescent sand.

Understanding IRC’s Requirements

We recognize the importance of self-charging phosphorescent systems for illuminating large areas with latrines. These systems enhance safety by providing constant lighting, which is crucial for women’s safety at night. Our proposed solution aims to illuminate both the inside and surrounding areas of latrines, addressing concerns of theft and vandalism. While there is no one-size-fits-all solution, our research and design offer a viable and sustainable lighting solution for refugee camps

Proper lighting around latrines and throughout the camp increases safety and prevents theft. Our design ensures the panels are large enough to be impractical to conceal and carry. Lighting maintenance and security are challenging, so our efforts focus on broader areas for efficiency.

A significant concern for community toilets is theft. The designed prototype panels are securable, deterring theft, and large enough to be visible during daytime charging. Camps with 300-3000+ people and specific clusters of women's latrines can minimize costs while making latrines safer to use at night. WASH reports indicate that 40% of women do not use the provided latrines, highlighting the need for improved solutions.

<u>Focusing on lighting both inside and around the latrines is crucial. To avoid theft, the light source needs to be impractical to conceal and carry at night. It is also important to ensure all tents and the local community in the camp vicinity benefit from the same system. Lighting the area surrounding the latrines is as important as lighting the latrines themselves. There are significant positive impacts related to protection issues in refugee camps that justify this approach. Lighting maintenance and security are challenging, so efforts should focus on the broader area rather than just the latrine for efficiency.</u>

Lighting only the latrines without addressing the surrounding areas and paths of the camp will not solve the problem, especially if women's latrines are far from the tents or clustered separately. Camps with 300-3000+ people and 200 tents would require at least 200 panels besides the latrines. Proper lighting inside and around latrines and throughout the camp, including tents and local communities, increases safety and prevents theft. Large panels that are lockable with simple mechanisms deter theft. Reports indicate that only 50% of women use the latrines at night, likely an underestimation.

While there is always an optimal solution, it might not be the right one. After reviewing discussions since 2012 about illuminating refugee camps and emergencies, we understand the issue's persistence. Other methods have failed to provide an inclusive and sustainable lighting solution for several reasons. Discussions about gravity lights, solar-charged LED lanterns, and crank-charged systems indicate these are meant for individual use, not for lighting large areas with latrines. If phosphorescent panels are broadly available and installed throughout the camp in various dimensions, they offer a real solution for all beneficiaries. Lighting the surroundings of toilets with support from the refugee committee ensures night-time safety. The committee can designate young people for night shifts to monitor and ensure camp safety.

Our proposed panel and the prototype we created is feasible, similar to polymer-embedded products that are ubiquitously sold as pathway and garden lights. We understand why the IRC and stakeholders seek self-charging phosphorescent systems to illuminate large areas with latrines rather than alternative solutions like beacons and gravity lights. **For women's safety and to make latrines safer to use at night, large phosphorescent panel installations with constant lighting are essential. Solutions that involve turning LEDs on and off can alert assailants, making users more vulnerable, especially if the latrine is not constantly illuminated.**

While there is no one-size-fits-all solution, our research and design offer a viable and sustainable lighting solution for refugee camps. By integrating phosphorescent panels into latrines, we can achieve the necessary illumination levels while meeting cost constraints and addressing security concerns. This approach ensures the safety and well-being of camp residents, particularly women, by providing consistent and reliable lighting in and around latrines.